Long-duration effect of multi-factor stresses on the cellular biochemistry, oil-yielding performance and morphology of *Nannochloropsis oculata*

Likun Wei[1], **Xuxiong Huang**[1,2,3]*

1 Key Laboratory of Genetic Resources for Freshwater Aquaculture and Fisheries, College of Fisheries and Life Science, Shanghai Ocean University, Shanghai, China, **2** Shanghai Engineering Research Centre of Aquaculture, Shanghai, China, **3** Shanghai University Knowledge Service Platform, Shanghai Ocean University Aquatic Animal Breeding Centre (ZF1206), Shanghai, China

* xxhuang@shou.edu.cn

Abstract

Microalga *Nannochloropsis oculata* is a promising alternative feedstock for biodiesel. Elevating its oil-yielding capacity is conducive to cost-saving biodiesel production. However, the regulatory processes of multi-factor collaborative stresses (MFCS) on the oil-yielding performance of *N. oculata* are unclear. The duration effects of MFCS (high irradiation, nitrogen deficiency and elevated iron supplementation) on *N. oculata* were investigated in an 18-d batch culture. Despite the reduction in cell division, the biomass concentration increased, resulting from the large accumulation of the carbon/energy-reservoir. However, different storage forms were found in different cellular storage compounds, and both the protein content and pigment composition swiftly and drastically changed. The analysis of four biodiesel properties using pertinent empirical equations indicated their progressive effective improvement in lipid classes and fatty acid composition. The variation curve of neutral lipid productivity was monitored with fluorescent Nile red and was closely correlated to the results from conventional methods. In addition, a series of changes in the organelles (e.g., chloroplast, lipid body and vacuole) and cell shape, dependent on the stress duration, were observed by TEM and LSCM. These changes presumably played an important role in the acclimation of *N. oculata* to MFCS and accordingly improved its oil-yielding performance.

Introduction

Microalgae are a diverse group of microorganisms with various unique biological characteristics, including high photosynthetic energy transfer efficiency, high biomass productivity, excellent adaptability to various environments and capability of producing a broad variety of bioenergy [1–3]. For example, the members of *Nannochloropsis* genus are marine Eustigmatophyceae microalgae with advantages such as fast growth and easy cultivation, capable of storing large triacylglycerols (TAGs) under particular culture conditions and are therefore an

environmentally friendly biodiesel feedstock with great developmental potential [4]. However, microalgae biodiesel still faces many problems in commercial production, such as high oil-yielding species to be screened or constructed, and technological innovations in large-scale cultivation, harvesting, oil extraction and transesterification of biolipids to biodiesel [1].

Increasing the oil-yielding capacity of microalgae is one of the keys to reduce the production cost of microalgae biodiesel, by improving both metabolic efficiency in lipid biosynthesis pathways and biomass productivity of microalgae [5]. There has been progress in increasing the lipid biosynthesis capability of microalgae through high biomass cultivation, metabolic engineering and genetic engineering [6–8]. To increase fatty acid (FA) biosynthesis, genetic engineering regulating cell metabolic pathways is feasible, including the over-expression or inhibition of certain rate-limiting enzymes [7–9], the comprehensive regulation of lipid biosynthesis by transcription factors [10], the construction of genes in association with spontaneous secretion of FA and the construction of efficient expression vectors for exogenous genes [3].

Metabolic pathway regulation, however, is relatively easy to undertake, the nature of which is to expose microalgae to environmental stresses, thus resulting in cellular metabolic flux with a shift to lipid biosynthesis [3, 6]. Microalgae have evolved countermeasures for survival in the face of various environmental adversities [6, 11]. The adaptation generated can quickly become evident as variations in their growth, physiology, biochemistry and morphology. However, high diversity of microalgae may well lead to the differences in cellular metabolic pathways and metabolic regulation between different species [6, 12, 13]. It is therefore possible to regulate many physiological metabolic processes in microalgae by changing their culture conditions, to obtain the end products or intermediate products of algal cells, such as proteins, FAs, pigments and polysaccharides.

By the orthogonal experiments of both multi-factor and multi-level stresses, we obtained the optimal culture conditions for *N. oculata* with a high TL content [14]. However, little information is available on the regulatory processes of multi-factor collaborative stresses (MFCS) on the oil-yielding performances of *N. oculata*. This study continued to adapt the optimal culture method for metabolic regulation of *N. oculata*. We explored the variations in growth, cellular biochemistry, FA and TAG production, biodiesel property and morphology of *N. oculata* during MFCS (i.e., high irradiation, nitrogen deficiency, and elevated iron supplementation). A rapid and high-throughput method using Nile red (NR) staining for monitoring neutral lipid (NL) in *N. oculata* was established; we dynamically detected the relative content of NL, and quickly and effectively determined the optimal harvest period to obtain the highest lipid productivity. Through LSCM and TEM, we synthetically observed the variations in the lipid bodies and cellular ultrastructure of *N. oculata* during the stresses, which confirmed the lipid accumulation process.

Materials and methods

Culture of microalgae

Nannochloropsis oculata was provided by the Culture Collection of Microalgae at Shanghai Ocean University. This microalgal strain was first axenically cultivated in 60-L photobioreactors under favourable conditions: f/2 culture medium, correct nutrient concentrations, 20 of salinity, 25°C, 150 $\mu mol \cdot m^{-2} \cdot s^{-1}$ of continuous irradiation, and 0.2 vvm of continuous sterile aeration.

When NO_3-N concentration in the microalgal suspension as described above was lower than 2 mg $N \cdot mL^{-1}$ (12.32 mg $N \cdot mL^{-1}$ in f/2 medium), it was supposed to be in nitrogen deficiency conditions. *N. oculata* was then immediately and directly exposed to optimal culture

conditions for lipid storage: 360 μmol·m^{-2}·s^{-1} of continuous elevated irradiation and 6.72 mg Fe·L^{-1} of elevated ferric citrate supplementation. This combined light-nitrogen-iron stress had been demonstrated as effectively regulating lipid metabolism in *N. oculata* [14]. In addition, this process does not use the conventional centrifugation-resuspension method and thus saves energy. Microalgae were cultivated in their original 60-L photobioreactors (60 L of actual liquid volume) for an 18-d duration and were kept in circular flow with the help of a mini-submersible pump and water-circulating pipe. Other culture conditions at that moment were 6.185×10^7 cells·mL^{-1} of microalgal cell density, 20‰ of salinity, 20°C, 1.45±0.07 mg N·mL^{-1} of NO$_3$-N concentration, 0.24±0.00 mg P·mL^{-1} of total phosphorus concentration, and 0.2 vvm of continuous sterile aeration.

Growth performances

Microalgal cell density and biomass concentration were determined everyday by haemocytometer and gravimetric methods, respectively. First, 20–40 mL (V) of microalgal suspension was filtered through an 0.44 μm pre-weighed cellulose acetate membrane (W$_0$), then cleaned by an equivalent volume of deionized water (pH = 4), and finally dried at 105°C until a constant weight (W$_1$). After that, the biomass concentration was determined as (g·L^{-1} DW) = (W$_1$−W$_0$)/V.

Assays of pigment, protein and sugar

The contents of pigment, protein and sugar were determined every other day in accordance with Pruvost's method [15]. Pigment (e.g., chl *a* and carotenoids) contents were obtained by spectrophotometric methods and total sugar content was determined by phenol-sulphuric acid method. To assay protein content, 4 mL of microalgal culture was harvested and re-suspended in 1 mL NaOH at 2 mol·L^{-1}. The samples were placed at 95°C for 10 mins and then neutralized by adding 1 mL HCL of 1.6 mol·L^{-1}. The supernatant obtained by centrifugation was used to analyse protein content by the Folin-phenol method.

Lipid analysis

Enough microalgal suspension was harvested by centrifugation and washed 3 times with deionized water (pH = 4). The cell pellets were then freeze-dried into powder at −46°C in preparation for the determination of lipid analysis every other day.

Total lipid (TL) content was determined by the chloroform-methanol (2:1, v/v) method [16]. The fatty acid (FA) profile was analysed by Aglient 7890A-5975C GC-MS using the direct transesterification method [17]. Lipid class compositions were assayed by a thin layer chromatography–flame ionization detector (TLC-FID) method. First, the dried TL was dissolved in moderate chloroform at 10–20 mg·mL^{-1}. The solution was then spotted into a silicon rod (10 mm×0.32 mm) for chromatography, which was then subjected to an outspread procedure with a solvent system of n-hexane-ether-formic acid (42:28:0.3, v:v:v). After drying, the silicon rod was used for analysis by IATROSCAN MK-6s (IATRON LABORATORIES INC., Japan). The resulting chromatogram was processed with Chormstar (IATRON) according to the qualitative analysis of the standard substances from Sigma for phospholipids (PLs), triacylglycerols (TAGs), diacylglycerol, monoacylglycerol, free FA, and cholesterol. Finally, the area normalization method was adopted to calculate the relative proportions of lipid classes.

Evaluation of biodiesel properties

According to previous studies, there exist mathematically relational models between the molecular structure and profile of fatty acid methyl ester (FAME) and biodiesel properties

[18]. Therefore, we can predict the properties of microalgal biodiesel (i.e., viscosity, iodine value, cetane number, and cold filter plugging point) by the relevant empirical equations below, helpful for evaluating whether it is an alternative to fossil fuel.

The 3 specific parameter definitions are:

Relative chain length (RCL),

$$\text{RCL} = \sum N_i \times P_i; \tag{1}$$

Saponification value (SV, mg KOH·g^{-1} oil),

$$SV = \sum (560 \times P_i)/MW_i; \tag{2}$$

Long chain saturated factor (LCSF),

$$LCSF = 0.1 \times P_{C16:0} + 0.5 \times P_{C18:0} + P_{C20:0} + 1.5 \times P_{C22:0} + 2 \times P_{C24:0}. \tag{3}$$

The formulae of the 4 prediction models are:

Viscosity (Vis, mm^2·s^{-1}) [19],

$$Vis = -1.72955 + 0.31247 \times \text{RCL} + 0.04228 \times P_{C22:1}; \tag{4}$$

Iodine value (IV, g I_2·$100g^{-1}$ oil) [20],

$$IV = \sum (254 \times m \times P_i)/MW_i; \tag{5}$$

Cetane number (CN) [21],

$$CN = 46.3 + 5458/SV - 0.225 \times IV; \tag{6}$$

Cold filter plugging point (CFPP, ˚C) [22],

$$CFPP = 3.1417 \times LCSF - 16.477. \tag{7}$$

For these formulae, *i*, *N*, *m*, *P*, and *MW* indicate certain FAME, the carbon chain length of FAME, the double bond number of FAME, the relative percentage content of FAME (% total FAMEs), and the molecular weight of FAME, respectively.

Nile red staining and quantification of neutral lipids

Nile red (NR) staining conditions optimized for *N. oculata* were as follows. The final solution was 3 mL, containing a certain volume of microalgal suspension, 0.5 ug/mL of NR, and 15% (v:v) of DMSO. The microalgal cell density in the final solution was diluted to 1.0×10^7 cells·mL^{-1}, or keeping its original state (6.0–8.5×10^7 cells·mL^{-1}), both situations of them taken into account. The solution was then incubated at 40˚C for 10 mins before determinations. If

the lipid content was very high when in the original state, the staining time was extended to 15 mins.

After the pre-treatment as described above, the fluorescence intensity (FI) of cellular neutral lipids (NLs) in the solution stained with NR was determined every day using a Fluorescence Spectrophotometer (HITACHI F-4600 FL). Its parameter settings were 523 nm of excitation wavelength, and 578 nm of emission wavelength. Eventually, the relative content of NL was expressed as FI (arbitrary units, a.u.) for each day, in line with its value under 1.0×10^7 cells·mL^{-1} of stained microalgal suspension. The relative productivity of NL was equal to the quotient of FI under $6.0–8.5 \times 10^7$ cells·mL^{-1} divided by the stress duration. The maximal volumetric NL productivity was considered as an indicator of the optimal harvest period for the microalgae.

Lipid bodies microexamination and cellular ultrastructure

Intracellular lipid bodies (LBs) stained with NR were microscopically observed by LSCM (ZEISS LSM 710) every other day. In addition, to observe the cellular ultrastructures at different stress durations (day 0, 4, 8, 12, 14, 16, and 18), an appropriate quantity of microalgal cell pellet was involved in a series of bio-specimen preparation procedures before observed by TEM (PHILIP CM-120), including fixation, dehydration, clearing, impregnation, embedding, trimming, cutting and staining.

Data analysis and processing

All sample indices underwent parallel determinations 3 times. The results were expressed as the means±SD, and analysed using one-way ANOVA and Duncan's new multiple-range test for statistical significance by PASW Statistics18.0 at a significance level $P < 0.05$. Images from LCSM and TEM were processed by their accessory image processing systems. In addition, the correlation and regression analyses between FI and the results obtained from lipid analyses were also conducted, as well as the variance analysis of the regression model.

Results

Cell growth performance

Microalgal cells began to grow slowly after day 3 (Fig 1). Biomass concentration was not significantly different from days 3–9 or days 11–18 ($P > 0.05$). Cell density on day 14 (8.351×10^7 cells·mL^{-1}, the maximum value) increased by 35.0% compared to the initial value (6.185×10^7 cells·mL^{-1}), while biomass concentration increased by 75.6% correspondingly (from 0.344 g·L^{-1} to 0.604 g·L^{-1}), presumably due to the increased cellular volume and cellular specific gravity observed from microscopy. The storage carbon/energy reservoir in a single cell therefore seemed to increase. It was thus evident that *N. oculata* retained the ability to grow slowly during a short period of environmental stress.

Cellular biochemistry variation

The photosynthetic pigments of *N. oculata* were mainly chl *a* and carotenoids, with the initial values accounting for 84.86% and 15.14% of total pigments, respectively (Fig 2B and 2D). The carotenoids proportion (% total pigments) on day 18 increased by 72.5% compared to its initial value, but it was the opposite for chl *a*. As a result, the colour of the algal cell suspension gradually changed from green to yellow (Fig 2F). Chl *a* content (% DW) declined substantially under MFCS, as did carotenoids (Fig 2A and 2C). Finally, the total pigment content (% DW) on day 18 decreased by 80.96% compared to the initial value (Fig 2E).
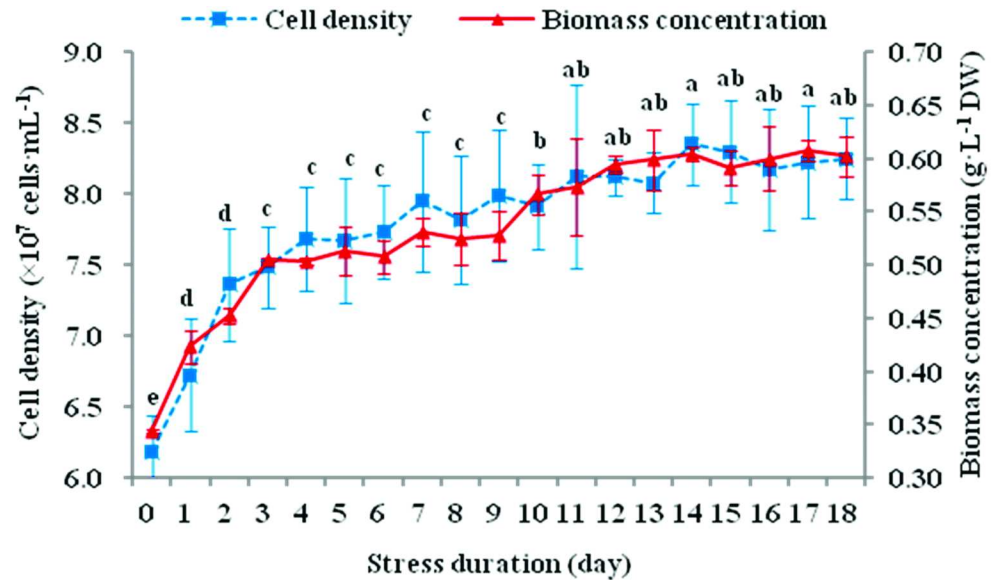
Fig 1. Variation in the cell growth of *N. oculata* during long-term MFCS. *N. oculata* was cultured axenically in 60-L photobioreactors with continuous sterile aeration, under multi-factor collaborative stress (MFCS; i.e., 360 µmol·m^{-2}·s^{-1} of high irradiation, nitrogen deficiency and 6.72 mg Fe·L^{-1} of iron supplementation). The cell density and biomass concentration represent the cell growth performances of *N. oculata* in quantity and weight, respectively. Different small letters for biomass concentration denote significant differences among different stress durations at *P*<0.05. (means±SD of three replicates).

TL (% DW) showed an increasing trend, from 28.52% to 49.14% on day 18 (Fig 3A). The protein content (% DW) declined remarkably during the first 2 d of MFCS and then decreased continuously, from 32.10% to 13.76% on day 18 (Fig 3B). Interestingly, the total sugar content (% DW) increased from 10.73% to 12.82% on day 4, but then fluctuated between 12.37% and 13.59% (Fig 3C).

Lipid class composition, FA profile, and biodiesel properties

Similar to the TL content, the TAG proportion (% TL) increased from 8.85% to 78.16% on day 18, while the phospholipid (PL) proportion decreased from 84.97% to 20.60%, and the other minor lipid classes (i.e., diacylglycerol, monoacylglycerol, free FA and cholesterol) proportions all underwent a significant decline (Fig 4A).

The FA profiles of *N. oculata* mainly contained 16:0, 16:1n7, 18:1n9, 20:5n3 (eicosapentaenoic acid, EPA), and 20:4n6 (arachidonic acid, ARA) (Table 1), similar to the majority species of the Eustigmatophyceae [23]. Along with the stresses, the proportions of saturated FA (SFA) and monounsaturated FA (MUFA) (% total FA) gradually increased, from a sum of 63.56% to 92.18%, while the polyunsaturated FA (PUFA, including EPA and ARA) proportion increasingly declined, from 21.29% to 4.12%. Conceivably, if the culture had continued after day 18, the reduction in PUFA proportions might have continued. As in the previous nitrogen-iron-temperature combined culture experiment, the EPA proportion could finally drop as low as 1% [14]. In particular, both the proportion (% total FA, Table 1) and absolute content (mg·g^{-1} DW, S1 Table) of 16:0 increased, as well as that of 18:1n9, which suggests that they play a conspicuous role in the course of TAG reserve. In addition, the total FA content (i.e., biodiesel yield) increased from 110.21 to 261.94 mg·g^{-1} (Table 1).

The productivities of TAG and biodiesel reached the maximums of 14.83 and 9.94 mg·L^{-1}·d^{-1} on day 10 and 12, respectively (Fig 4B), which could be a reference for the best time to harvest.
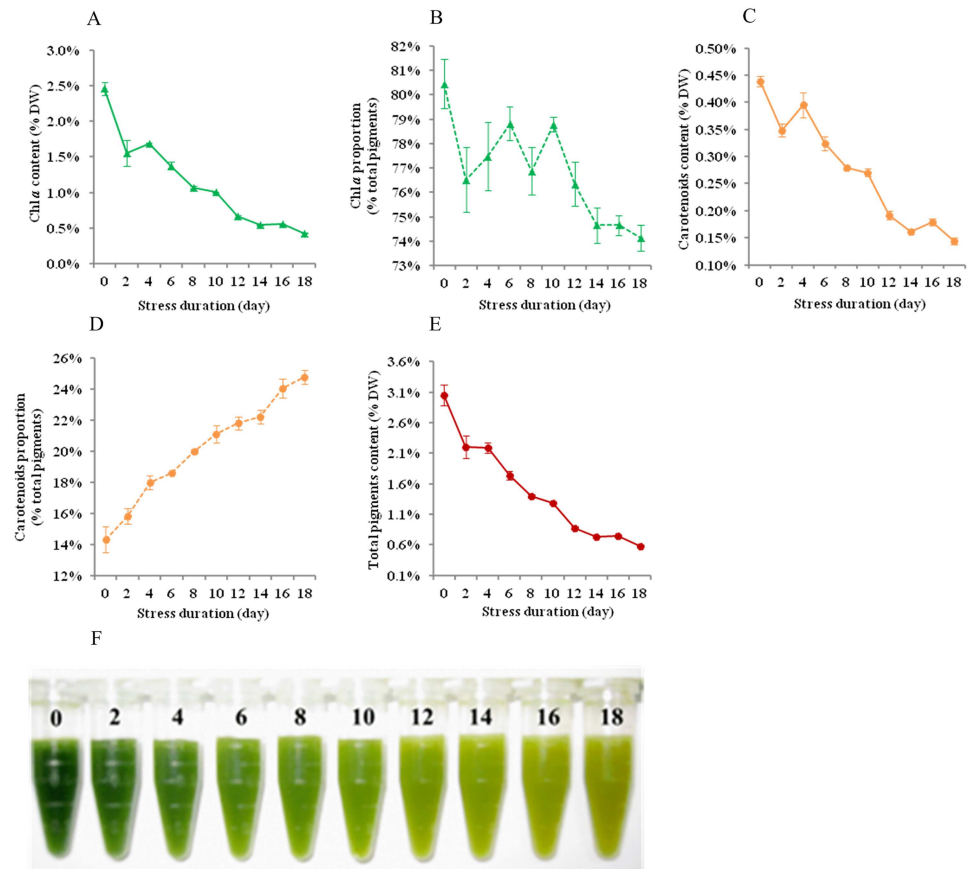
Fig 2. Variations in the pigment contents and cell suspension colour of *N. oculata* during long-term MFCS. MFCS means multi-factor collaborative stresses (i.e., 360 μmol·m^{-2}·s^{-1} of high irradiation, nitrogen deficiency and 6.72 mg Fe·L^{-1} of iron supplementation). The solid lines denote the absolute contents (% DW) of chl *a* (A), carotenoids (C) and total pigments (E). The dotted lines denote the relative contents (% total pigments) of chl *a* (B) and carotenoids (D). (F) Colour changes of *N. oculata* suspension, concentrated 5 times by centrifugation (5 mL re-suspended in 1 ml); the numbers denote the stress duration (day). (means ±SD of three replicates).

Based on the pertinent empirical equations as described in the experimental procedures, the variation in the biodiesel properties of *N. oculata* during MFCS could be predicted (Table 2). Both Vis (3.46–3.72 mm^2·s^{-1}) and CFPP (−5.65 to −1.31˚C) could meet the biodiesel standards of the USA and the European Union throughout the culture period, while IV (72.67–156.80 g·100g^{-1}) and CN (38.76–56.88) could meet the standards after day 4 and increasingly improved as the MFCS continued (Table 2 and S2 Table).

Relative content and relative productivity of NL

The fluorescence intensity (FI) of microalgal cells stained with NR was distinct in different stress durations (Fig 5). The relative content of neutral lipid (NL), that is FI, was drastically augmented as the stress progressed, reaching its peak on day 15, and had no significant differences during days 15–20. It was basically consistent with the results obtained from traditional gravimetric methods [16] (see Lipid analysis in Materials and methods), such as TL content (maximum 49.47% DW, day 16) and TAG content (maximum 38.61% DW, day 16). The relative productivity of NL showed a tendency to increase at first and then to decrease, and
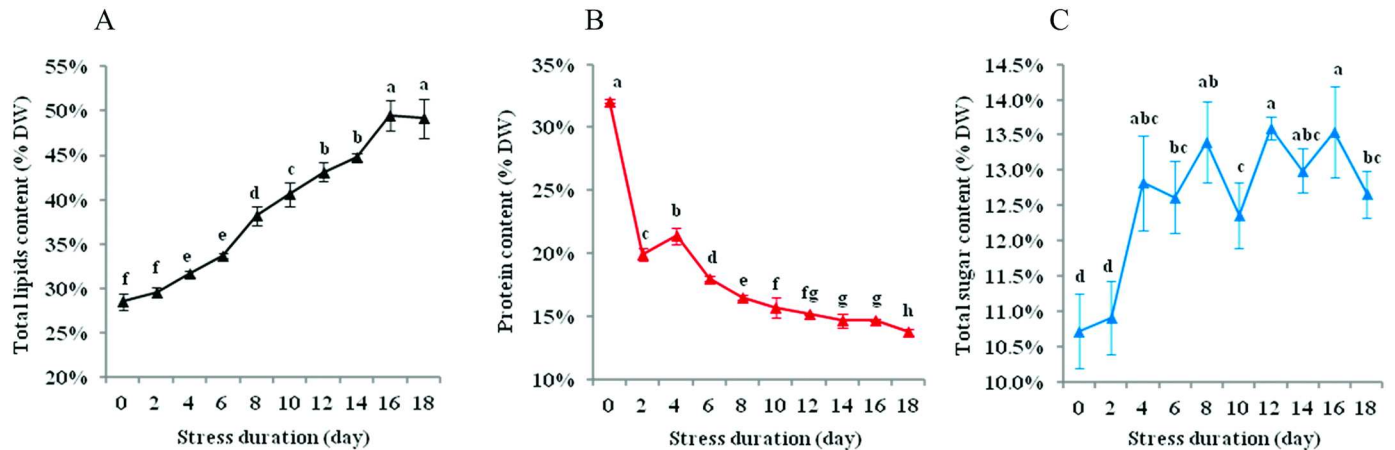
Fig 3. Content variations in the total lipids (A), protein (B) and total sugar (C) of *N. oculata* during long-term MFCS. MFCS means multi-factor collaborative stresses (i.e., 360 μmol·m^{-2}·s^{-1} of high irradiation, nitrogen deficiency and 6.72 mg Fe·L^{-1} of iron supplementation). Different small letters in one panel denote significant differences among different stress durations at *P*<0.05. (means±SD of three replicates).

reached its maximum during days 10–13 (Fig 5). It was compatible with TAG productivity (maximum 14.83 mg·L^{-1}·d^{-1}, day 10) and biodiesel productivity (maximum 9.94 mg·L^{-1}·d^{-1}, day 12) (Fig 4B).

The FI of microalgal cells stained with NR had significant linear positive correlations with TL content or yield obtained by the chloroform-methanol method [16], the TAG content or yield obtained by the TLC-FID method, and the biodiesel yield obtained by the GC-MS method [17], with correlation coefficients between 0.971–0.997, *P*<<0.01 (Table 3). Similarly, the regression equations had high fitting degrees, with determination coefficients of 0.944–0.993, *P*<<0.01. Therefore, by determining the FI of microalgal cells stained with NR, it might comparatively accurately estimate the oil-yielding capacity of *N. oculata* by means of relevant linear regression equations.

Cellular lipid bodies and ultra-microstructure

N. oculata accumulated lipids in the form of lipid bodies (LBs), also called lipid droplet. The LBs of *N. oculata* stained with NR gave a strong yellow fluorescence by LSCM, while the chloroplasts showed a red auto-fluorescence (Fig 6). As a result, in situ specific fluorescent staining of living cells made it easy to locate the LBs of *N. oculata*. The fluorescence of the LBs was first captured on day 6 (Fig 6D), with 33.70% DW of TL content. Then, the accumulation rate of cellular lipids was augmented. Meanwhile, the number and size of the LBs in a single cell gradually increased, as well as its FI. However, only a single large yellow fluorescent spot could be observed in most *N. oculata* cells (Fig 6J). Nevertheless, the FI and the size of chloroplast decreased step by step. Thus, the cellular lipids of *N. oculata* gradually increased during MFCS, which was consistent with the results obtained by the gravimetric method.

As shown by TEM, *N. oculata* cells had a spherical or oval shape, a diameter of approximately 2–4μm, a thin cell wall, an oval or cupulate chloroplast, several mitochondria, and a nucleus (Fig 7). In addition, pyrenoids or starch granules were not found. The average cellular volume increased somewhat after stress cultivation, but no thickening of the cell wall was observed.

With stress, the size and number of LBs in most cells increased progressively, filling the majority of the cellular space. Some of them merged into one large LB in a cell, resulting in an
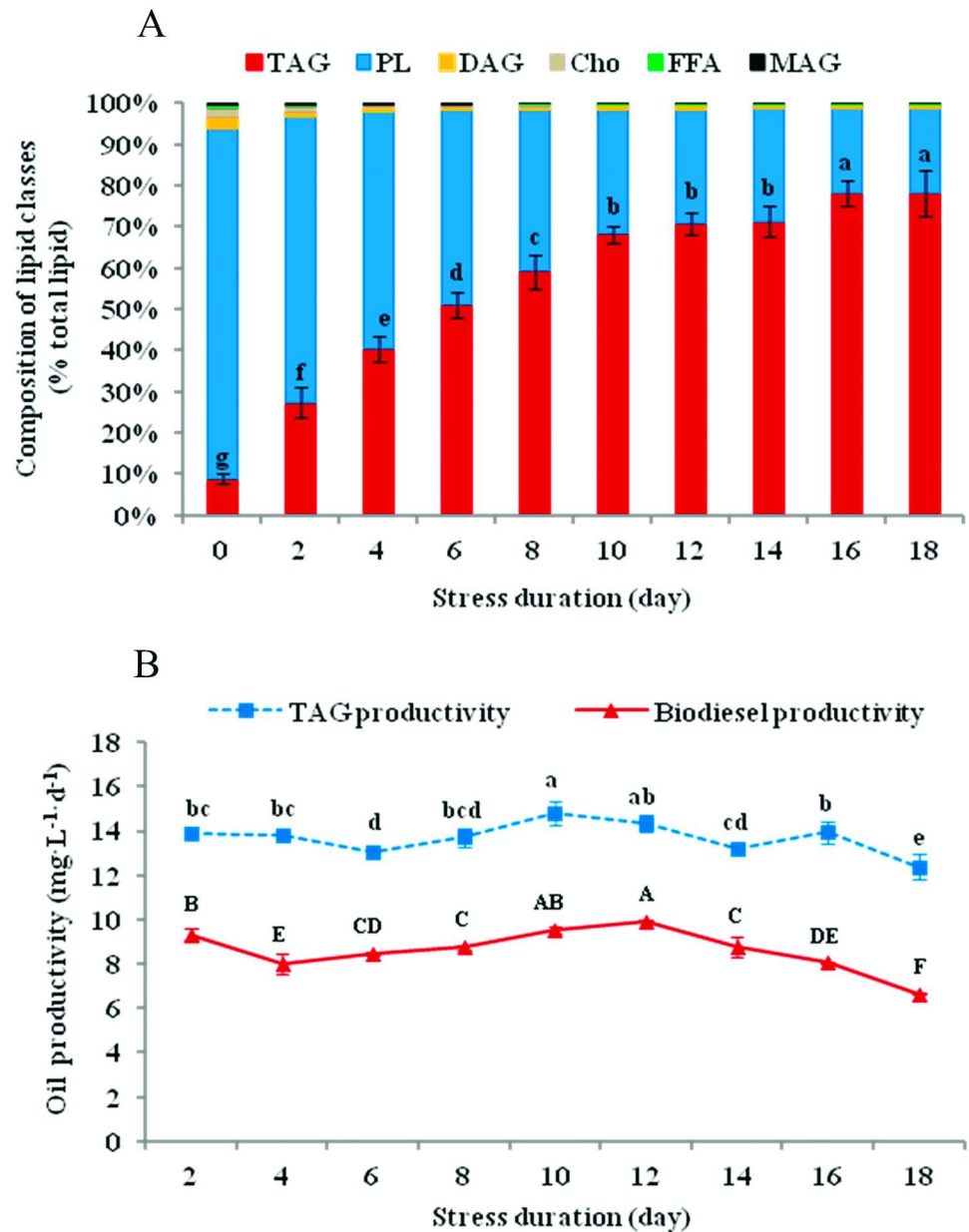
Fig 4. Variations in the lipid classes composition (a) and oil productivity (b) of *N. oculata* during long-term MFCS. MFCS means multi-factor collaborative stresses (i.e., 360 µmol·m^{-2}·s^{-1} of high irradiation, nitrogen deficiency and 6.72 mg Fe·L^{-1} of iron supplementation). TAG, triacylglycerol; PL, phospholipid; DAG, diacylglycerol; Cho, cholesterol; FFA, free fatty acids; MAG, monoacylglycerol. Biodiesel productivity indicates the productivity of total fatty acid methyl esters. See S1 Fig for the neutral and polar lipid compositions included in this analysis. Different small or capital letters in one panel denote significant differences within the same type of letter among different stress durations at *P*<0.05. (means±SD of three replicates).

increasingly full cell. The cross-sectional area of the LBs made up approximately 60–70% of that of one single cell on day 18, and the diameter of the LB was 0.5–2µm (Fig 7G). This reflected the TL accumulation process of *N. oculata* during the course of MFCS. The long striped thylakoids were clearly visible and ran through the chloroplast at the beginning of the

Table 1. Variation in the fatty acid profile of *N. oculata* during long-term MFCS.

Fatty acids (% total FA)	Stress duration (day)									
	0	2	4	6	8	10	12	14	16	18
14:0	3.22 ±0.26a	2.67 ±0.12bc	2.84±0.62b	3.12 ±0.24a	2.82±0.08b	2.58 ±0.08bc	2.53±0.07c	2.62±0.11bc	2.58 ±0.08bc	2.55±0.24c
16:0	24.06 ±0.54g	32.41 ±1.28f	36.43 ±1.73e	40.01 ±0.46d	41.11 ±0.39abc	40.68 ±0.21bcd	41.57 ±0.68a	41.39 ±0.61ab	40.48 ±0.24cd	41.11 ±0.24abc
16:1n7	26.64 ±1.23d	28.91 ±2.14abc	28.54 ±2.63abc	26.80 ±0.35d	28.04 ±0.24c	29.27 ±0.34ab	29.05 ±0.69abc	28.27 ±0.43bc	28.29 ±0.34bc	29.66 ±1.06a
18:0	2.08 ±0.02a	1.37 ±0.04cd	1.38 ±0.07cd	1.43 ±0.12cd	1.38 ±0.10cd	1.36 ±0.06cd	1.46±0.09bc	1.46±0.13bc	1.56 ±0.06b	1.31±0.12d
18:1n9	5.78 ±0.08g	8.38±0.79f	8.44±0.23f	10.57 ±0.33e	12.28 ±0.32d	14.10 ±0.39c	14.43 ±0.51c	15.49±0.22b	16.60 ±0.12a	16.47 ±0.11a
18:2n6	5.46 ±0.01a	3.86±0.35b	4.15±1.16b	2.71±0.06c	2.26±0.03d	1.98±0.06d	1.64±0.12e	1.59±0.18e	1.61 ±0.04e	1.46±0.12e
ARA	9.69 ±0.60a	7.20±0.04b	5.81±0.68c	4.98 ±0.23d	3.91±0.18e	3.06±0.10f	2.94±0.17fg	2.93±0.09fg	2.74 ±0.06g	2.25±0.24h
EPA	21.29 ±0.10a	13.36 ±0.14b	10.70 ±0.24c	8.73 ±0.26d	6.73±0.29e	5.63±0.24f	5.19±0.24g	5.04±0.26g	4.95 ±0.21g	4.12±0.65h
Others	1.79 ±0.17ab	1.84±0.08a	1.72 ±0.23bc	1.64±0.08c	1.47±0.04d	1.35±0.04e	1.20±0.02f	1.20±0.04f	1.19±0.10f	1.08±0.03g
∑16C	50.70 ±0.69i	61.32 ±0.86h	64.97 ±0.91g	66.81 ±0.73f	69.15 ±0.35de	69.95 ±0.53bc	70.62 ±0.01ab	69.67 ±0.60cd	68.77 ±0.10e	70.77 ±0.81a
∑18C	13.32 ±0.09g	13.61 ±0.48hg	13.96 ±0.86h	14.71 ±0.50f	15.91 ±0.32e	17.43 ±0.48d	17.53 ±0.48d	18.54±0.43c	19.76 ±0.22a	19.24 ±0.13b
∑20C	30.98 ±0.51a	20.56 ±0.18b	16.50 ±0.92c	13.72 ±0.49d	10.64 ±0.36e	8.69±0.21f	8.13±0.40g	7.97±0.34g	7.70 ±0.14g	6.36±0.89h
∑SFA	30.42 ±0.67d	37.69 ±1.54c	41.91 ±2.68b	45.85 ±0.42a	46.47 ±0.40a	45.69 ±0.26a	46.50 ±0.66a	46.44±0.44a	45.58 ±0.28a	45.83 ±0.16a
∑MUFA	33.14 ±1.18f	37.90 ±1.37e	37.44 ±2.44e	37.72 ±0.47e	40.63 ±0.53d	43.64 ±0.18c	43.73 ±1.19c	44.01±0.55c	45.11 ±0.18b	46.35 ±1.17a
∑PUFA	36.44 ±0.50a	24.42 ±0.17b	20.65 ±0.24c	16.43 ±0.49d	12.90 ±0.33e	10.67 ±0.20f	9.77±0.53g	9.56±0.48g	9.30 ±0.10g	7.82±1.01h
∑FAMEs*	110.21 ±0.50h	125.20 ±5.07g	138.95 ±16.32f	174.83 ±2.78e	205.81 ±5.98d	235.54 ±7.45c	264.51 ±0.53ab	266.63 ±25.86ab	277.90 ±1.93a	261.94 ±0.64b

Note: MFCS means multi-factor collaborative stresses (i.e., 360 µmol·m^{-2}·s^{-1} of high irradiation, nitrogen deficiency and 6.72 mg Fe·L^{-1} of iron supplementation). Other FAs (i.e., others in this table) are C12:0, C15:0, C17:0 and C17:1n7, all of whose contents are less than 1% of total FAs. ARA, arachidonic acid (C20:4n6); EPA, eicosapentaenoic acid (C20:5n3); SFA, saturated FA; MUFA, monounsaturated FA; PUFA, polyunsaturated FA.
* The unit of ∑FAMEs is mg·g^{-1} DW. See S1 Table for the absolute quantification of FA profile (mg·g^{-1} DW). Different superscript letters in the same row denote significant differences at $P<0.05$. (means±SD of three replicates).

experiment (Fig 7A). As the stress progressed, the volume of the chloroplast apparently decreased (Fig 7D), and the thylakoid structure was increasingly fuzzy and eventually disintegrated, as well as other organelles (Fig 7G). Moreover, vacuoles began to emerge from day 4.

Discussion

Pigment alteration

Nannochloropsis is a promising source of commercially valuable pigments [24]. Its pigment composition is mostly Chl *a* with a small amount of carotenoids under favourable conditions. The adjustment of pigment composition is a mechanism for microalgae to adapt to environmental stresses [9, 25, 26]. Both high irradiation and nitrogen deficiency can cause cell

Table 2. Variation in the biodiesel properties of *N. oculata* during long-term MFCS.

Biodiesel properties	Stress duration (day)									
	0	2	4	6	8	10	12	14	16	18
Vis (mm^2·s^{-1})	3.72±0.00[a]	3.60±0.00[b]	3.55±0.00[c]	3.51±0.01[d]	3.48±0.00[e]	3.47±0.01[e]	3.46±0.00[ef]	3.47±0.01[e]	3.47±0.00[e]	3.45±0.01[f]
IV (gI$_2$·100g^{-1})	156.80±0.41[a]	118.49±1.28[b]	103.41±1.21[c]	90.49±1.52[d]	80.84±1.03[e]	75.91±0.77[f]	73.23±0.61[g]	72.67±1.20[g]	72.71±0.74[g]	68.68±2.49[h]
CN	38.76±0.08[h]	46.97±0.31[g]	50.19±0.27[f]	52.99±0.32[e]	55.07±0.22[d]	56.14±0.16[c]	56.73±0.13[b]	56.87±0.25[b]	56.88±0.17[b]	57.72±0.51[a]
CFPP (°C)	-5.65±0.20[f]	-4.14±0.47[e]	-2.87±0.65[d]	-1.66±0.15[c]	-1.39±0.17[abc]	-1.57±0.05[bc]	-1.13±0.07[a]	-1.18±0.10[a]	-1.31±0.16[ab]	-1.51±0.26[bc]

Note: MFCS means multi-factor collaborative stresses (i.e., 360 µmol·m^{-2}·s^{-1} of high irradiation, nitrogen deficiency and 6.72 mg Fe·L^{-1} of iron supplementation). The estimation of four biodiesel properties was based on the pertinent empirical equations from the fatty acid methyl esters profile. Vis, viscosity; IV, iodine value; CN, cetane number; CFPP, cold filter plugging point. Different superscript letters in the same row of each treatment denote significant differences at $P<0.05$. (means±SD of three replicates).

yellowing (Fig 2F) by reducing chlorophyll content and increasing carotenoids proportion simultaneously (Fig 2A, 2C and 2D). One reason for that is the large amount of reactive oxygen species (ROS) generated under environmental stresses [27]. This is because pigments, especially chlorophyll, are very sensitive to oxidation reactions. However, carotenoids can protect against oxidative stress and dissipate excess excitation energy [28]. Another reason is that
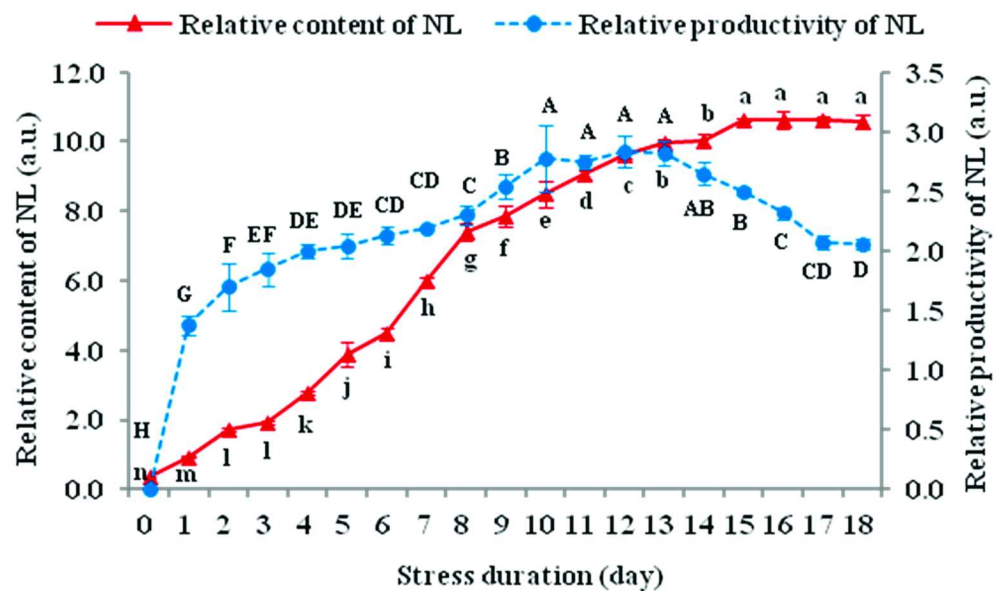

Fig 5. Variations in the relative content and relative productivity of Neutral Lipids (NLs) in *N. oculata* during long-term MFCS. MFCS means multi-factor collaborative stresses (i.e., 360 µmol·m^{-2}·s^{-1} of high irradiation, nitrogen deficiency and 6.72 mg Fe·L^{-1} of iron supplementation). The relative content of NL was represented by the fluorescence intensity (FI, a.u.) of cellular NL stained with Nile red in each day, as the stained *N. oculata* suspension was diluted to a cell density of 1.0×10^7 cells·mL^{-1}. The relative productivity of NL was represented by the quotient of FI in each day divided by stress duration, as the stained *N. oculata* suspension was at its original cell density of 6.0–8.5×10^7 cells·mL^{-1}. See S2 Fig for details on the relative production of NL included in this analysis. Different small letters for relative content of NL and capital letters for relative productivity of NL mean significant differences within the same type of letter among different stress durations at $P<0.05$. (means±SD of three replicates).

Table 3. Regression results of the oil-yielding capacity and fluorescence intensity of cellular neutral lipids in *N. oculata* using Nile red staining.

Regression variables	Regression equations	r	R^2	Sig.
TL content [a] (% DW)	y = 0.0193x + 0.2612	0.971	0.944 (0.936)	0.00000284
TAG content [a] (% DW)	y = 0.0316x + 0.0216	0.986	0.972 (0.969)	0.00000016
Biodiesel yield [a] (mg·g^{-1} DW)	y = 16.325x + 98.289	0.994	0.987 (0.986)	0.00000001
TL yield [b] (mg·L^{-1})	y = 4.6346x + 102.69	0.987	0.975 (0.971)	0.00000012
TAG yield [b] (mg·L^{-1})	y = 5.3286x + 6.0908	0.987	0.974 (0.971)	0.00000012
Biodiesel yield [b] (mg·L^{-1})	y = 3.2342x + 38.003	0.997	0.993 (0.993)	0.00000000

Note: The superscripts a and b, respectively, indicate the fluorescence intensity (FI, a.u.) used in the regression analysis from the values at cell densities of 1.0×10^7 and $6.0–8.5 \times 10^7$ cells·mL^{-1} in the stained *N. oculata* suspension. r, correlation coefficient; R^2, determination coefficient; TL, total lipids; TAG, triacylglycerols; Biodiesel yield, total FAMEs yield. The letter x and y in the regression equations, respectively, indicate the value of FI and the relevant regression variables. The values in the brackets of R^2 column denote the adjusted R^2.

chlorophyll, which is rich in nitrogen, can be degraded heavily under nitrogen starvation (Figs 2 and 7), thus providing a nitrogen source for cell metabolism and biomass accumulation. Therefore, *N. oculata* started to enter the plateau phase until day 4 and the decline phase was yet to come on day 18 (Fig 1). Jiang *et al.* [29] also found similar results. However, confronted with the prolonged lack of nitrogen resources, the synthesis of nitrogen compounds, such as nucleic acid and protein, will be restricted and thus affect biomass production.

The content changes of total lipids, protein and total sugar

MFCS could regulate *N. oculata* metabolism over a short duration (i.e., 4–12 d): more carbon was distributed into carbohydrates and lipids, protein synthesis was blocked and growth was limited (Figs 1 and 3). Carbohydrate metabolism was active—total sugar content increased at first, but then fluctuated within a small range (Fig 3C). While lipids have a higher energy density than carbohydrates, carbohydrates would be further converted into lipids by central carbon metabolism (e.g., TCA cycle) when carbohydrate reserves reach a certain threshold. It thus indicates that there are differential storage purposes between carbohydrates and lipids in some microalgae, carbohydrates as the preferentially synthesized and mobilized reserve and lipids representing long term storage in case of prolonged stress [2, 30]. In addition, the substantial degradation of cellular protein in *N. oculata* under MFCS (Fig 3B) may benefit the remobilization and redistribution of cellular nitrogen, such as the transformation from non-essential proteins to essential proteins, similar to the findings reported by Nicola Louise *et al.* [31] and Li *et al.* [32].

When cultured in favourable conditions (e.g., standard f/2 medium), *N. oculata* has a lipid content of about 25% (DW) [33]. This study and our high irradiation experiment (unpublished) found that both high light and nitrogen deficiency (more likely) collaboratively enhanced the lipid accumulation in *N. oculata*. High light can remodel the metabolite allocation in *Nannochloropsis* cells, especially for primary carbon partitioning between cell organelles. Such a regulation triggers a strong accumulation of TAGs in endoplasmic reticulum at the expensive of chloroplast, together with the up-regulation of genes involved in lipid biosynthesis [34, 35]. It is generally believed that under high light stress, excess electrons, produced by the electron transport chain in photosynthesis, will trigger the overproduction of ROS, thus limiting photosynthesis [27]. Yet, *de novo* FA synthesis can consume excess electrons, thereby alleviating photo-inhibition and photo-damage [28]. Thus, the amassing of TAGs is a mechanism used by some microalgae to adapt to high light stress [25, 36–38]. Many studies show that a high concentration of iron ions can promote not only the efficiencies of chlorophyll
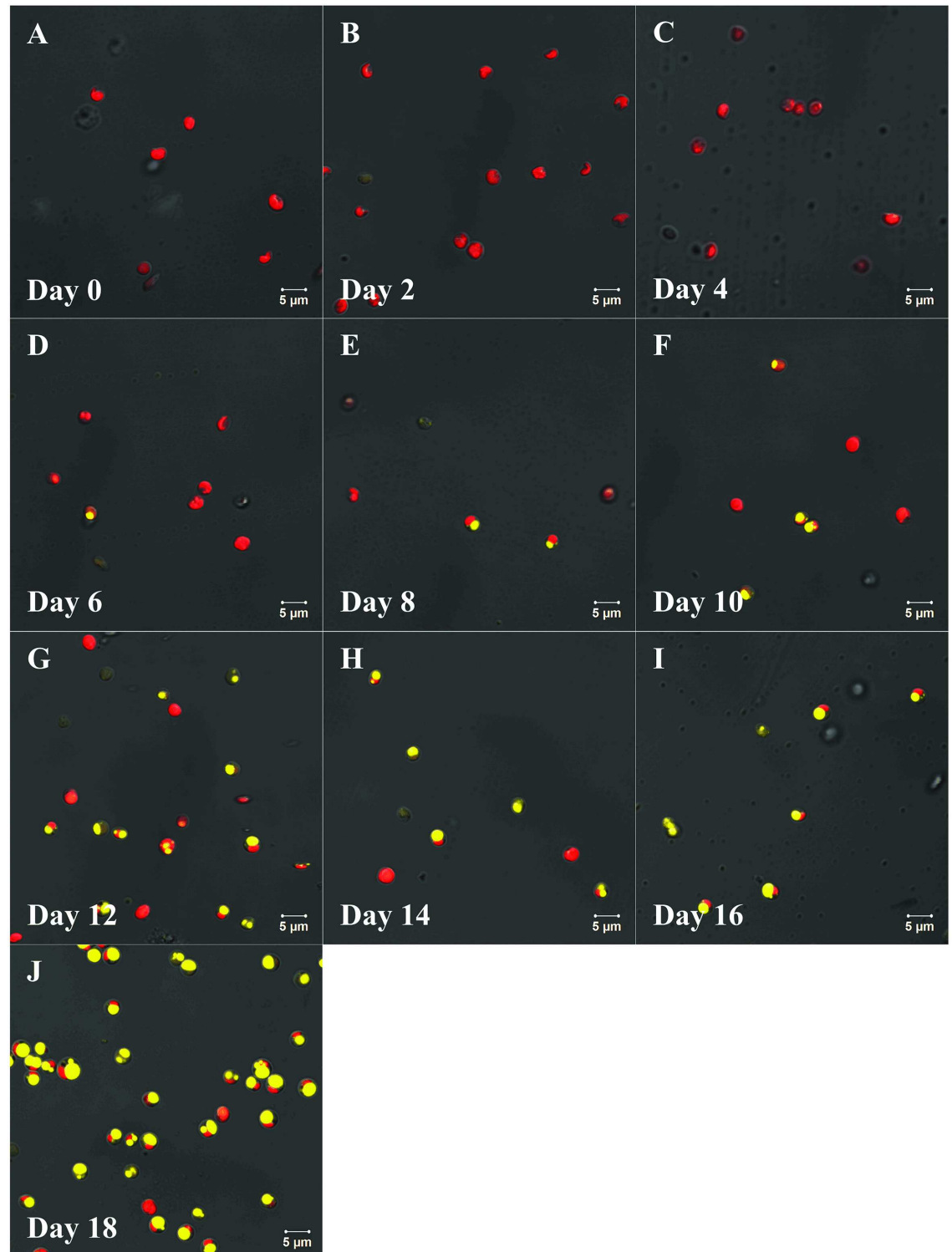
Fig 6. The intensity variation of intracellular lipid bodies stained with Nile red confirmed the lipid accumulation in *N. oculata* during long-term MFCS. This presents the confocal laser scanning micrographs (1260×) of *N. oculata* during multi-factor collaborative stresses (MFCS; i.e., 360 μmol·m^{-2}·s^{-1} of high irradiation, nitrogen deficiency and 6.72 mg Fe·L^{-1} of iron supplementation). (a)–(j), the micrographs on day 0 to 18. The intracellular chloroplast and lipid body show red auto-fluorescence and yellow fluorescence, respectively. Scale bars = 5 μm.

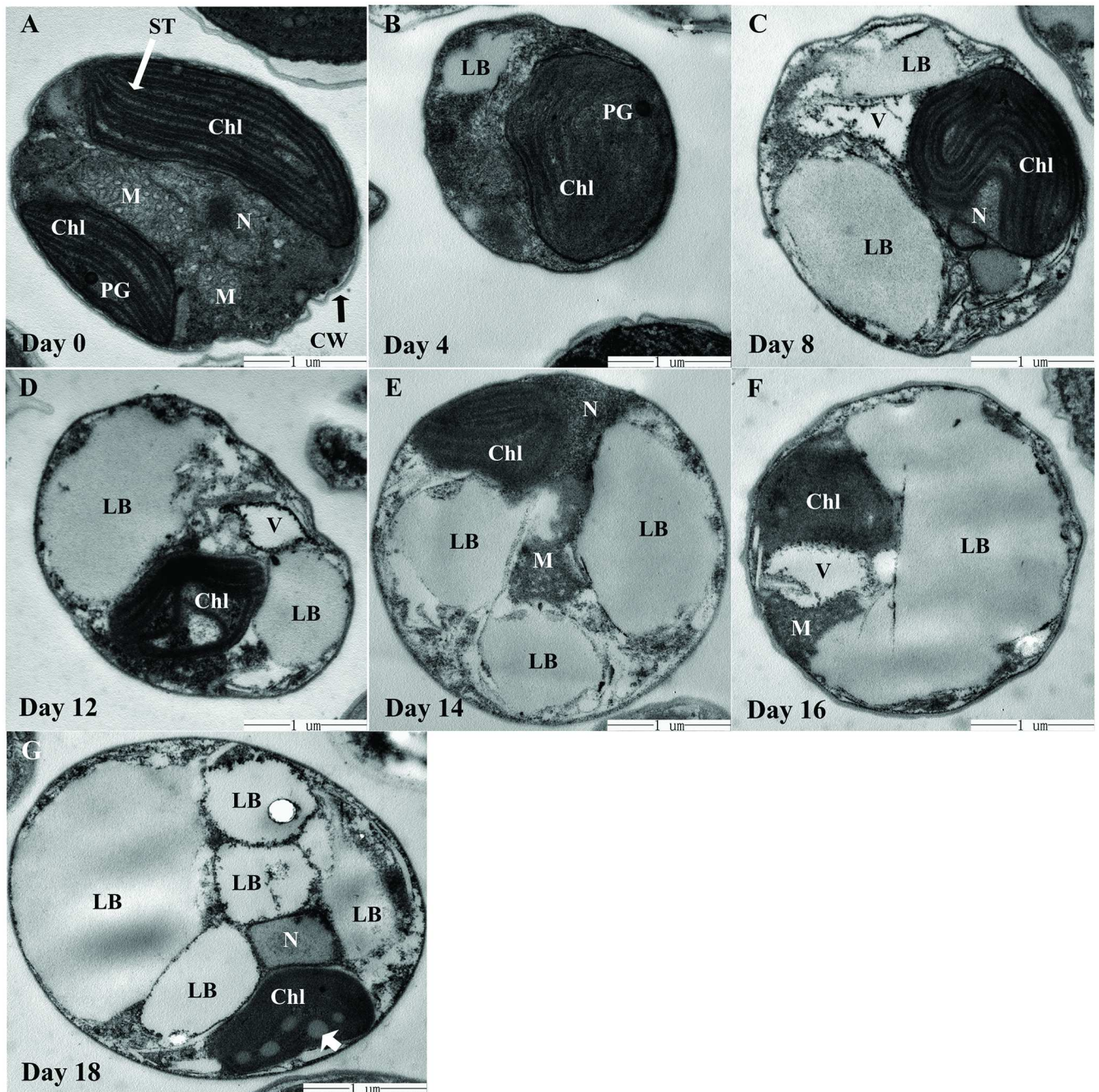**Fig 7. Cellular ultrastructure variation of *N. oculata* during long-term MFCS.** This presents the transmission electron micrographs (23000×) of *N. oculata* during multi-factor collaborative stresses (MFCS; i.e., 360 µmol·m^{-2}·s^{-1} of high irradiation, nitrogen deficiency and 6.72 mg Fe·L^{-1} of iron supplementation). (a), the cell on day 0 with few lipid bodies and normal organelle shape, including distinct stacks of thylakoids in chloroplast. (b), minute lipid bodies begin to emerge. (c), lipid bodies enlarge and large vacuoles are developed to degrade macromolecules. (d), (e), the obvious atrophy and degradation of chloroplast and other organelles; the accumulation of lipid bodies results in an increasingly full and round cell. (f), the fusion of some lipid bodies into a larger one. (g), several large lipid bodies oppress the protoplast content onto the cell wall on day 18; the poor chloroplast structure with impaired thylakoid membranes and small primary lipid bodies in the chloroplast (arrowhead). LB, lipid body; Chl, chloroplast; N, nucleus; M, mitochondrion; V, vacuole; PG, plastoglobulus; ST, stacks of thylakoids; CW, cell wall. Scale bars = 1 µm.

synthesis and photosynthesis but also lipid accumulation [14, 33, 39]. According to the nitrogen-iron-temperature combined culture experiment, *N. oculata* under 6.72 mg Fe·L^{-1} had a high TL content (53%) and the highest lipid production (142 mg·L^{-1}) [14]. There are direct action sites for iron in the electron transport chains in chloroplasts and mitochondria, which affect photosynthesis and respiration, thus affecting carbon storage and lipid reserves [33, 39].

Lipid class composition, FA profile, and biodiesel properties

High NL content (mainly TAGs) is an important advantage for microalgae as biodiesel feedstock [8]. There is a low content ratio of NL/PL for *N. oculata* under non-stressful conditions [14, 33]. As the stresses progressed, the NL proportion of *N. oculata* increased dramatically (Fig 4A and S1 Fig). Microalgae can rapidly remobilize TAG reserves stored in LBs for cell proliferation in a more favourable environment; for example, nitrogen replenishment triggers LB degradation [26, 40]. In addition, there were 8.83 times as many TAGs proportionally on day 18 as in the beginning, while the other lipid classes decreased correspondingly (Fig 4A). Perhaps there are ways for redundant PLs or other lipid classes to transform into TAGs [7].

Nitrogen deficiency can result in the declining generation of chloroplasts, which leads to lower demands for membrane structural components (e.g., PLs and glycerolipids) rich in PUFA [14, 26, 30, 41]. In this study, the PUFA proportion gradually declined as the stress progressed, while the proportions of SFA and MUFA increased accordingly, their sum increasing from 63.56% to 92.18% (Table 1). The FA profile of *N. oculata* cells here is the opposite of that under non-stressful conditions [14, 33]. Excessive high light can result in the oxidative damage of PUFA, but promote the synthesis of SFA beneficial to consume excess photo-energy to alleviate photo-damage [28, 38]. Both C16:0 and C18:1, for example, are important precursors of TAG synthesis [42], and their proportions and absolute contents all remarkably increased (Table 1 and S1 Fig).

Microalgae biodiesel exhibits excellent properties in environmental protection, lubrication, low-temperature start-up and renewability [1]. However, little is known about the effect of environmental stresses on the properties of microalgae biodiesel. In view of the effect of FA profile on CFPP and IV, both SFA and PUFA in biodiesel should be as low as possible [43]. Biodiesel feedstock with high quality should have a high MUFA content, especially straight-chain C16 or C18 MUFA [44]. In this study, as the stress progressed, the proportions of SFA and MUFA increased, while the PUFA proportion decreased (Table 1). These changes, therefore, resulted in the significant improvement of IV and CN (Table 2). However, the augmentation of SFA proportion led to somewhat poor CFPP, which still met the biodiesel standards in relevant countries (S2 Table). This study indicated that environmental stresses could benefit the properties of *N. oculata* biodiesel.

The use of fluorescent Nile red for neutral lipid measurement

Previous reports often qualitatively describe lipids by the NR staining method [45–47]. By combining the conventional methods and the fluorometric staining using NR, this study identified linear regression equations with high goodness of fit between FI and the oil-yielding performance indexes (i.e., TL content, TAG content, and biodiesel production) (Table 3). As a result, we could apply these equations in the quantification determination of oil-yielding performances of *N. oculata* at different growth phases during MFCS, without need of pre-concentration.

The results obtained in this novel way were comparable to those determined by traditional methods (Table 3). This approach is easy, real-time and economic for microalgae NL quantification compared with conventional gravimetric methods which require approximately 0.2g

dry biomass of microalgae to determine lipid content [16]. Furthermore, multifunctional fluorescent ELISA can be used in this method for the large-scale screening of oleaginous microalgal strains and the optimization of culture conditions.

Cellular ultramicrostructural changes

The LBs were 0.5–2μm in diameter (Fig 7), similar to the reports for plant seeds and algae [29]. The LBs of *N. oculata* were relatively independent, stable and integrated in shape. As the stresses progressed, the LBs gradually filled most of the cell space and the cell became plump, which is similar to the findings of Jiang *et al.* [29]. Surface proteins of LBs (e.g., oleosin), abundant in microalgae and plant seeds, could help maintain the stability and integrity of LB shape [40] and may participate in cell signal transmission, stress response and lipid metabolism [48]. The ontogeny of LBs is not very clear so far. It is thought that LBs, as TAG deposit, are firstly generated by two lobes of the endoplasmic reticulum, and then develop into a discontinuous organelle, attached or not to the endoplasmic reticulum membrane [49].

Autophagy is a vital pathway for plants to recycle cytoplasmic contents in the vacuoles upon environmental stress [26, 50]. *N. oculata* generated large vacuoles containing membranous inclusions and isolated organelles (Fig 7C and 7F). Therefore, the cellular destruction of *N. oculata* could be related to the autophagy induced by MFCS. We found that thylakoid membrane degradation occurred in *N. oculata* (Fig 7), in agreement with the results from the chemical extraction method (Fig 2, reduced chlorophyll level). Both Yang *et al.* [51] and Iwai *et al.* [42] reported the similar findings. This result may imply the progressive decline of the chlorophyll antenna size to adapt to environmental stresses.

Our study provides evidence that MFCS could significantly promote the oil-yielding performance of *N. oculata* in a short duration (i.e., 4–12 d). This will help reveal its adaptation mechanisms to environmental stresses, and better understand the manipulation of metabolic pathway to enhance the production of algal oil in oleaginous microalgae.

Supporting information

S1 Fig. Variations in the neutral and polar lipid compositions of *N. oculata* during long-term MFCS. MFCS means multi-factor collaborative stresses (i.e., 360 $\mu mol \cdot m^{-2} \cdot s^{-1}$ of high irradiation, nitrogen deficiency and 6.72 mg $Fe \cdot L^{-1}$ of iron supplementation). NL, neutral lipid; PL, polar lipid. Different small letters for neutral lipid column denote significant differences among different stress durations at $P < 0.05$. (means±SD of three replicates).
(TIF)

S2 Fig. Variations in the relative content and relative production of cellular Neutral Lipids (NLs) in *N. oculata* during long-term MFCS. MFCS means multi-factor collaborative stresses (i.e., 360 $\mu mol \cdot m^{-2} \cdot s^{-1}$ of high irradiation, nitrogen deficiency and 6.72 mg $Fe \cdot L^{-1}$ of iron supplementation). The relative quantification of NL was represented by the fluorescence intensity (FI, a.u.) of cellular NL stained with Nile red in each day, as the stained *N. oculata* suspension was diluted to a cell density of 1.0×10^7 cells·mL^{-1} (for the relative content of NL) or being at its original cell density of 6.0–8.5×10^7 cells·mL^{-1} (for the relative production of NL). Different small letters for the relative content of NL mean significant differences among different stress durations at $P < 0.05$. (means±SD of three replicates).
(TIF)

S1 Table. Variation in the fatty acid profile of *N. oculata* during long-term MFCS.
(DOCX)

S2 Table. Quality items of biodiesel standards in different countries.
(DOCX)

Acknowledgments

We would like to thank Mr. Hao Wu from Shanghai Ocean University for the GC-MS analysis of FA, and Dr. Jie Yang and Dr. Qin Hang from Shanghai Jiao Tong University for making the TEM preparation, electron micrographs and confocal micrographs.

Author Contributions

Conceptualization: XXH.

Data curation: LKW XXH.

Formal analysis: LKW.

Funding acquisition: XXH.

Investigation: LKW.

Methodology: LKW XXH.

Project administration: LKW XXH.

Resources: XXH.

Software: LKW.

Supervision: XXH.

Validation: LKW XXH.

Visualization: LKW XXH.

Writing – original draft: LKW.

Writing – review & editing: LKW XXH.

References

1. Malcata FX. Microalgae and biofuels: a promising partnership? Trends in biotechnology. 2011; 29 (11):542–9. https://doi.org/10.1016/j.tibtech.2011.05.005 PMID: 21724282

2. Liu B, Benning C. Lipid metabolism in microalgae distinguishes itself. Current opinion in biotechnology. 2013; 24(2):300–9. https://doi.org/10.1016/j.copbio.2012.08.008 PMID: 22981869

3. Levering J, Broddrick J, Zengler K. Engineering of oleaginous organisms for lipid production. Current Opinion in Biotechnology. 2015; 36:32–9. https://doi.org/10.1016/j.copbio.2015.08.001 PMID: 26319892

4. Kilian O, Benemann CS, Niyogi KK, Vick B. High-efficiency homologous recombination in the oil-producing alga *Nannochloropsis* sp. Proceedings of the National Academy of Sciences. 2011; 108 (52):21265–9.

5. Peers G. Increasing algal photosynthetic productivity by integrating ecophysiology with systems biology. Trends in biotechnology. 2014; 32(11):551–5. https://doi.org/10.1016/j.tibtech.2014.09.007 PMID: 25306192

6. Gimpel JA, Henríquez V, Mayfield SP. In Metabolic Engineering of Eukaryotic Microalgae: Potential and Challenges Come with Great Diversity. Frontiers in Microbiology. 2015; 6(e42949).

7. Merchant SS, Kropat J, Liu B, Shaw J, Warakanont J. TAG, You're it! Chlamydomonas as a reference organism for understanding algal triacylglycerol accumulation. Current opinion in biotechnology. 2012; 23(3):352–63. https://doi.org/10.1016/j.copbio.2011.12.001 PMID: 22209109

8. Ahmad I, Sharma AK, Daniell H, Kumar S. Altered lipid composition and enhanced lipid production in green microalga by introduction of brassica diacylglycerol acyltransferase 2. Plant biotechnology journal. 2015; 13(4):540–50. https://doi.org/10.1111/pbi.12278 PMID: 25403771

9. Shtaida N, Khozingoldberg I, Solovchenko A, Chekanov K, Didicohen S, Leu S, et al. Downregulation of a putative plastid PDC E1α subunit impairs photosynthetic activity and triacylglycerol accumulation in nitrogen-starved photoautotrophic *Chlamydomonas reinhardtii*. Journal of Experimental Botany. 2014; 65(65):6563–76.

10. Matthijs M, Fabris M, Broos S, Vyverman W, Goossens A. Profiling of the Early Nitrogen Stress Response in the Diatom *Phaeodactylum tricornutum* Reveals a Novel Family of RING-Domain Transcription Factors. Plant Physiology. 2016; 170(1):489–98. https://doi.org/10.1104/pp.15.01300 PMID: 26582725

11. Blaby IK, Glaesener AG, Mettler T, Fitz-Gibbon ST, Gallaher SD, Liu B, et al. Systems-level analysis of nitrogen starvation–induced modifications of carbon metabolism in a *Chlamydomonas reinhardtii* starchless mutant. The Plant Cell. 2013; 25(11):4305–23. https://doi.org/10.1105/tpc.113.117580 PMID: 24280389

12. Pfeil BE, Schoefs B, Spetea C. Function and evolution of channels and transporters in photosynthetic membranes. Cellular & Molecular Life Sciences. 2014; 71(6):979–98.

13. Wagner H, Jakob T, Wilhelm C. Balancing the energy flow from captured light to biomass under fluctuating light conditions. New Phytologist. 2006; 169(1):95–108. https://doi.org/10.1111/j.1469-8137.2005.01550.x PMID: 16390422

14. Wei LK, Huang XX, Huang ZZ, Zhou ZG. Orthogonal test design for optimization of lipid accumulation and lipid property in *Nannochloropsis oculata* for biodiesel production. Bioresource Technology. 2013; 147(0):534–8. http://dx.doi.org/10.1016/j.biortech.2013.08.079.

15. Pruvost J, Van Vooren G, Le Gouic B, Couzinet-Mossion A, Legrand J. Systematic investigation of biomass and lipid productivity by microalgae in photobioreactors for biodiesel application. Bioresource technology. 2011; 102(1):150–8. https://doi.org/10.1016/j.biortech.2010.06.153 PMID: 20675127

16. Folch J, Lees M, Sloane-Stanley G. A simple method for the isolation and purification of total lipids from animal tissues. J biol Chem. 1957; 226(1):497–509. PMID: 13428781

17. Griffiths M, Van Hille R, Harrison S. Selection of direct transesterification as the preferred method for assay of fatty acid content of microalgae. Lipids. 2010; 45(11):1053–60. https://doi.org/10.1007/s11745-010-3468-2 PMID: 20820931

18. Westbrook CK. Biofuels Combustion*. Annual review of physical chemistry. 2013; 64:201–19. https://doi.org/10.1146/annurev-physchem-040412-110009 PMID: 23298249

19. Duan M. Optimization of biodiesel preparation form *Chlorella* oil. China: Zhejiang University; 2011.

20. Kalayasiri P, Jeyashoke N, Krisnangkura K. Survey of seed oils for use as diesel fuels. Journal of the American Oil Chemists' Society. 1996; 73(4):471–4.

21. Krisnangkura K. A simple method for estimation of cetane index of vegetable oil methyl esters. Journal of the American Oil Chemists Society. 1986; 63(4):552–3.

22. Ramos MJ, Fernández CM, Casas A, Rodríguez L, Pérez Á. Influence of fatty acid composition of raw materials on biodiesel properties. Bioresource Technology. 2009; 100(1):261–8. https://doi.org/10.1016/j.biortech.2008.06.039 PMID: 18693011

23. Kaye Y, Grundman O, Leu S, Zarka A, Zorin B, Didi-Cohen S, et al. Metabolic engineering toward enhanced LC-PUFA biosynthesis in *Nannochloropsis oceanica*: Overexpression of endogenous Δ12 desaturase driven by stress-inducible promoter leads to enhanced deposition of polyunsaturated fatty acids in TAG. Algal Research. 2015; 11:387–98.

24. Lubián LM, Montero O, Moreno-Garrido I, Huertas IE, Sobrino C, González-del Valle M, et al. Nannochloropsis (Eustigmatophyceae) as source of commercially valuable pigments. J Appl Phycol. 2000; 12(3):249–55.

25. Bhandari R, Sharma PK. High-light-induced Changes on Photosynthesis, Pigments, Sugars, Lipids and Antioxidant Enzymes in Freshwater (*Nostoc spongiaeforme*) and Marine (*Phormidium corium*) Cyanobacteria. Photochemistry and photobiology. 2006; 82(3):702–10. https://doi.org/10.1562/2005-09-20-RA-690 PMID: 16464127

26. Dong HP, Williams E, Wang DZ, Xie ZX, Hsia RC, Jenck A, et al. Responses of *Nannochloropsis oceanica* IMET1 to Long-Term Nitrogen Starvation and Recovery. Plant Physiology. 2013; 162(2):1110–26. https://doi.org/10.1104/pp.113.214320 PMID: 23637339

27. Apel K, Hirt H. Reactive oxygen species: metabolism, oxidative stress, and signal transduction. Annu Rev Plant Biol. 2004; 55:373–99. https://doi.org/10.1146/annurev.arplant.55.031903.141701 PMID: 15377225

28. Li Z, Wakao S, Fischer BB, Niyogi KK. Sensing and responding to excess light. Annual review of plant biology. 2009; 60:239–60. https://doi.org/10.1146/annurev.arplant.58.032806.103844 PMID: 19575582

29. Jiang P-L, Pasaribu B, Chen C-S. Nitrogen-Deprivation Elevates Lipid Levels in *Symbiodinium* spp. by Lipid Droplet Accumulation: Morphological and Compositional Analyses. PloS one. 2014; 9(1):e87416. https://doi.org/10.1371/journal.pone.0087416 PMID: 24475285

30. Recht L, Zarka A, Boussiba S. Patterns of carbohydrate and fatty acid changes under nitrogen starvation in the microalgae *Haematococcus pluvialis* and *Nannochloropsis* sp. Applied microbiology and biotechnology. 2012; 94(6):1495–503. https://doi.org/10.1007/s00253-012-3940-4 PMID: 22361859

31. Nicola Louise H, Thomas M, Francis M, Stanislav K, Gill M. The response of diatom central carbon metabolism to nitrogen starvation is different from that of green algae and higher plants. Plant Physiology. 2012; 158(1):299–312. https://doi.org/10.1104/pp.111.184333 PMID: 22065419

32. Li J, Han D, Wang D, Ning K, Jia J, Wei L, et al. Choreography of transcriptomes and lipidomes of *Nannochloropsis* reveals the mechanisms of oil synthesis in microalgae. The Plant Cell. 2014; 26(4):1645–65. https://doi.org/10.1105/tpc.113.121418 PMID: 24692423

33. Huang XX, Wei LK, Huang ZZ, Yan JQ. Effect of high ferric ion concentrations on total lipids and lipid characteristics of *Tetraselmis subcordiformis*, *Nannochloropsis oculata* and *Pavlova viridis*. J Appl Phycol. 2014; 26(1):105–14.

34. Alboresi A, Perin G, Vitulo N, Diretto G, Block MA, Jouhet J, et al. Light remodels lipid biosynthesis in nannochloropsis gaditana by modulating carbon partitioning between organelles. Plant Physiology. 2016:pp. 00599.2016.

35. Schulze PS, Pereira HG, Santos TF, Schueler L, Guerra R, Barreira LA, et al. Effect of light quality supplied by light emitting diodes (LEDs) on growth and biochemical profiles of Nannochloropsis oculata and Tetraselmis chuii. Algal Research. 2016; 16:387–98.

36. Goold HD, Cuiné S, Légeret B, Liang Y, Brugière S, Auroy P, et al. Saturating Light Induces Sustained Accumulation of Oil in Plastidal Lipid Droplets in Chlamydomonas reinhardtii. Plant physiology. 2016: pp. 00718.2016.

37. Yao L, Shen H, Wang N, Tatlay J, Li L, Tan TW, et al. Elevated acetyl-CoA by amino acid recycling fuels microalgal neutral lipid accumulation in exponential growth phase for biofuel production. Plant Biotechnology Journal. 2016.

38. Rosenberg JN, Kobayashi N, Barnes A, Noel EA, Betenbaugh MJ, Oyler GA. Comparative analyses of three *Chlorella* species in response to light and sugar reveal distinctive lipid accumulation patterns in the microalga *C. sorokiniana*. PloS one. 2014; 9(4):e92460. https://doi.org/10.1371/journal.pone.0092460 PMID: 24699196

39. Concas A, Steriti A, Pisu M, Cao G. Comprehensive modeling and investigation of the effect of iron on the growth rate and lipid accumulation of *Chlorella vulgaris* cultured in batch photobioreactors. Bioresource technology. 2014; 153:340–50. https://doi.org/10.1016/j.biortech.2013.11.085 PMID: 24389410

40. Goold H, Beisson F, Peltier G, Li-Beisson Y. Microalgal lipid droplets: composition, diversity, biogenesis and functions. Plant cell reports. 2015; 34(4):545–55. https://doi.org/10.1007/s00299-014-1711-7 PMID: 25433857

41. Huang XX, Huang ZZ, Wen W, Yan JQ. Effects of nitrogen supplementation of the culture medium on the growth, total lipid content and fatty acid profiles of three microalgae (*Tetraselmis subcordiformis*, *Nannochloropsis oculata* and *Pavlova viridis*). J Appl Phycol. 2013; 25(1):129–37.

42. Iwai M, Ikeda K, Shimojima M, Ohta H. Enhancement of extraplastidic oil synthesis in *Chlamydomonas reinhardtii* using a type-2 diacylglycerol acyltransferase with a phosphorus starvation–inducible promoter. Plant biotechnology journal. 2014; 12(6):808–19. https://doi.org/10.1111/pbi.12210 PMID: 24909748

43. Stansell GR, Gray VM, Sym SD. Microalgal fatty acid composition: Implications for biodiesel quality. J Appl Phycol. 2012; 24(4):1–11.

44. Knothe G. A comprehensive evaluation of the cetane numbers of fatty acid methyl esters. Fuel. 2014; 119(119):6–13.

45. Xie B, Stessman D, Hart JH, Dong H, Wang Y, Wright DA, et al. High-throughput fluorescence-activated cell sorting for lipid hyperaccumulating *Chlamydomonas reinhardtii* mutants. Plant biotechnology journal. 2014; 12(7):872–82. https://doi.org/10.1111/pbi.12190 PMID: 24702864

46. Rumin J, Bonnefond H, Saint-Jean B, Rouxel C, Sciandra A, Bernard O, et al. The use of fluorescent Nile red and BODIPY for lipid measurement in microalgae. Biotechnology for Biofuels. 2015; 8(1):1–16.

47. Greenspan P, Mayer EP, Fowler SD. Nile red: a selective fluorescent stain for intracellular lipid droplets. Journal of Cell Biology. 1985; 100(3):965–73. PMID: 3972906

48. Huang NL, Huang MD, Chen TL, Huang AH. Oleosin of subcellular lipid droplets evolved in green algae. Plant Physiology. 2013; 161(4):1862–74. https://doi.org/10.1104/pp.112.212514 PMID: 23391579

49. Wilfling F, Wang H, Haas J, Krahmer N, Gould T, Uchida A, et al. Triacylglycerol Synthesis Enzymes Mediate Lipid Droplet Growth by Relocalizing from the ER to Lipid Droplets. Developmental Cell. 2013; 24(4):384–99. https://doi.org/10.1016/j.devcel.2013.01.013 PMID: 23415954

50. Liu Y, Xiong Y, Bassham DC. Autophagy is required for tolerance of drought and salt stress in plants. Autophagy. 2009; 5(7):954–63. PMID: 19587533

51. Yang ZK, Niu YF, Ma YH, Jiao X, Zhang MH, Yang WD, et al. Molecular and cellular mechanisms of neutral lipid accumulation in diatom following nitrogen deprivation. Biotechnology for Biofuels. 2013; 6 (1):1–14.